w, 1844 w, 1843 w cm^{-1}. ^{1}H NMR: −17.0 ppm (q, $^1J_{Rh-H}$ = 12.0 Hz). Recrystallization from CH_2Cl_2 by slow evaporation of the solvent gave dark red air-stable crystals.

Crystallographic Studies. Data were collected on a Nicolet R3m diffractometer using Mo Kα radiation (λ = 0.71073 Å). Accurate cell parameters were obtained from 25 automatically centered reflections in the range 15° < 2θ < 35° and 8° < 2θ < 22° for 1 and 2, respectively. Intensities were corrected for background, polarization, and Lorentz factors. Empirical absorption corrections were made from ψ-scan data. Table VII presents further crystallographic information.

The metal atom positions were solved by direct methods with use of the SHELXTL program package.[18] All remaining non-hydrogen atoms were located by the usual combination of full-matrix least-squares refinement and difference electron density syntheses. Metal, sulfur, oxygen, and carbon atoms were anisotropically refined for both structures. Methyl protons were placed on idealized positions (C–H = 0.96 Å, U = 0.08 Å^2) and not refined.

Acknowledgment. We thank Dr. Outi Krause for helpful discussions. Neste Ltd. and the Academy of Finland are acknowledged for financial support.

Supplementary Material Available: Tables of anisotropic thermal parameters and bond lengths and angles for 1, 2, and $HRuCo_3(CO)_{10}(SMe_2)_2$[14] (11 pages); listings of structure factors (38 pages). Ordering information is given on any current masthead page.

---

[18] "SHELXTL Plus, Release 3.4"; Nicolet Co.: Madison, WI, 1988.

Ligand Behavior of the $[HRu_3(CO)_{10}(\mu\text{-}CO)]^-$ Cluster Anion toward a Borane: Synthesis of and Molecular and Electronic Structure of $[HRu_3(CO)_{10}(\mu\text{-}COBH_2NMe_3)]$

Ann K. Chipperfield, Catherine E. Housecroft,* and Paul R. Raithby

University Chemical Laboratory, Lensfield Road, Cambridge CB2 1EW, U.K.

Received May 17, 1989

The compound $[HRu_3(CO)_{10}(\mu\text{-}COBH_2NMe_3)]$ (1) has been obtained as a minor product from the reaction of $Ru_3(CO)_{12-x}(NCMe)_x$ (x = 1, 2) either with THF·BH_3 in the presence of NMe_3 or directly with $Me_3N{\cdot}BH_3$. The second boron-containing product is proposed from spectroscopic data to be $[Ru_6(CO)_{17}B][HNMe_3]$. The structure of 1 has been determined by single-crystal X-ray crystallography: monoclinic, $P2_1/c$, a = 14.938 (2) Å, b = 9.153 (1) Å, c = 16.872 (1) Å, β = 100.66 (1)°, V = 2267 Å^3, Z = 4, R_F = 2.44%. In 1, the $[HRu_3(CO)_{10}(\mu\text{-}CO)]^-$ anion formally functions as a base toward the borane; the observed bond length of the cluster μ-CO group (1.262 (4) Å) in 1 is longer than that of the corresponding bond in $[HRu_3(CO)_{10}(\mu\text{-}CO)]^-$. A Fenske–Hall quantum-chemical analysis of the bonding in 1 illustrates that the cluster–borane interaction is localized and results in subtle changes to the cluster bonding within the $[HRu_3(CO)_{10}(\mu\text{-}CO)]^-$ fragment.

We have previously reported that the reaction of $Ru_3(CO)_{12}$ with THF·BH_3 and Li[$BHEt_3$] in hexane solution leads to the formation of $Ru_3(CO)_9BH_5$.[1] However, the reaction is far from specific, and difficulties encountered in the separation of the products have encouraged us to explore other synthetic strategies. The bis(acetonitrile) derivative of ruthenium carbonyl $Ru_3(CO)_{10}(NCMe)_2$[2] appeared to be a potential precursor for Ru–B bond formation. The acetonitrile ligands are labile, and the compound has been used as an intermediate in the formation of several ruthenium-based clusters.[2] Here we illustrate that, in addition to the formation of the ruthenaboride cluster anion $[Ru_6(CO)_{17}B]^-$, the reaction of $Ru_3(CO)_{12-x}(NCMe)_x$ (x = 1, 2) with THF·BH_3 in the presence of NMe_3 leads to $[HRu_3(CO)_{10}(\mu\text{-}COBH_2NMe_3)]$, in which a bridging carbonyl ligand of the triruthenium cluster acts as a Lewis base toward the borane fragment. The formation of adducts between transition-metal carbonyl compounds, including $Ru_3(CO)_{12}$,[3] and group III alkyls and halides has been studied previously, and infrared spectroscopic data suggest that carbonyl ligand rearrangement may, in some cases, accompany adduct formation.[3]

Crystallographic characterization of transition-metal carbonyl–group III Lewis acid adducts is confined to the tricobalt species $Co_3(CO)_9(\mu_3\text{-}COBH_2NEt_3)$,[4] $Co_3(CO)_9(\mu_3\text{-}COBCl_2NEt_3)$,[5] and $Co_3(CO)_9(\mu_3\text{-}COBBr_2NEt_3)$.[6] In each compound, the bridging carbonyl ligand exhibits a lengthened C–O bond, in keeping with the donation of electron density from the carbonyl to the coordinated Lewis acid. We present here the synthesis and structural characterization of $[HRu_3(CO)_{10}(\mu\text{-}COBH_2NMe_3)]$ (1) as well as an investigation of the electronic structure of the complex. The extent to which the interaction of the bridging carbonyl ligand with the borane fragment affects the bonding within the triruthenium cluster fragment is examined.

Experimental Section

General Data. FT-NMR spectra were recorded on a Bruker WM 250 or AM 400 spectrometer. ^{1}H NMR shifts are reported

---

[1] Chipperfield, A. K.; Housecroft, C. E. *J. Organomet. Chem.* **1988**, *349*, C17.

[2] Drake, S.; Khattar, R. J. In *Organometallic Syntheses*; King, R. B., Eisch, J. J., Eds.; Elsevier: Amsterdam, 1988; Vol. 4, p 234.

[3] Kristoff, J. S.; Shriver, D. F. *Inorg. Chem.* **1974**, *13*, 499 and references therein.

[4] Klanberg, F.; Askew, W. B.; Guggenberger, L. J. *Inorg. Chem.* **1968**, *7*, 2265.

[5] Bätzel, V.; Müller, U.; Allmann, R. *J. Organomet. Chem.* **1975**, *102*, 109.

[6] Bätzel, V. *Z. Naturforsch.* **1976**, *31B*, 342.

Table I. Crystal Data for $[HRu_3(CO)_{10}(\mu\text{-}COBH_2NMe_3)]$ (1)

(a) Crystal Parameters	
mol formula	$C_{14}H_{12}BNO_{11}Ru_3$
mol wt (M_r)	684.27
cryst color and habit	orange rectangular block
cryst dimens, mm	0.20 × 0.34 × 0.51
temp, K	291 ± 2
cryst syst	monoclinic
space group	$P2_1/c$
a, Å	14.938 (2)[a]
b, Å	9.153 (1)
c, Å	16.872 (1)
β, deg	100.66 (1)
V, Å^3	2267
Z	4
D(calcd), g cm^{-3}	2.004
μ(Mo Kα), cm^{-1}	19.60
F(000)	1312
(b) Data Collection	
scan limits, deg	$5 \leq 2\theta \leq 50$
no. of rflns collected	4422
no. of indep rflns	3871
no. of obs rflns ($4\sigma(F_o)$)	3663
R(merge), %	1.3
T_{max}/T_{min}	1.24
decay, %	≤2
(c) Refinement	
$R(F)$, $R(wF)$, %	2.44, 3.24
Δ/σ(final)	0.13
$\Delta(\rho)_{max}$, e Å^{-3}	0.33
N_o/N_v	12.54
g ($w^{-1} = \sigma^2(F_o) + gF_o^2$)	0.003

[a] Unit cell parameters determined from least-squares fit of the angular settings of 46 reflections ($20 \leq 2\theta \leq 25°$).

Table II. Atomic Coordinates (×10^4) and Isotropic Thermal Parameters (Å^2 × 10^3) for 1

	x	y	z	U(eq)[a]
Ru(1)	7173 (1)	1092 (1)	4992 (1)	36 (1)
Ru(2)	8015 (1)	3432 (1)	4324 (1)	36 (1)
Ru(3)	6104 (1)	3034 (1)	3898 (1)	40 (1)
C(1)	8124 (3)	−21 (4)	5615 (2)	48 (1)
O(1)	8707 (3)	−659 (4)	5978 (2)	77 (1)
C(2)	6491 (3)	1405 (5)	5881 (3)	55 (1)
O(2)	6087 (3)	1535 (5)	6382 (3)	93 (2)
C(3)	6481 (3)	−534 (5)	4531 (3)	56 (2)
O(3)	6083 (3)	−1504 (4)	4233 (3)	92 (2)
C(4)	9290 (3)	3259 (5)	4694 (3)	51 (1)
O(4)	10052 (3)	3133 (5)	4918 (3)	87 (2)
C(5)	7877 (3)	5427 (5)	4735 (3)	53 (1)
O(5)	7818 (3)	6571 (4)	4963 (3)	87 (2)
C(6)	8086 (3)	4105 (4)	3272 (3)	51 (1)
O(6)	8131 (3)	4554 (4)	2652 (2)	78 (1)
C(7)	4882 (3)	2393 (5)	3885 (3)	50 (1)
O(7)	4144 (2)	2061 (4)	3874 (3)	78 (1)
C(8)	5949 (3)	4763 (6)	3233 (3)	59 (2)
O(8)	5885 (3)	5801 (5)	2867 (3)	90 (2)
C(9)	6109 (3)	4096 (5)	4884 (3)	53 (1)
O(9)	6065 (2)	4758 (4)	5449 (2)	77 (1)
C(10)	6204 (3)	1702 (5)	3020 (3)	50 (1)
O(10)	6206 (2)	878 (4)	2516 (2)	74 (1)
C(11)	7817 (2)	1301 (4)	4060 (2)	36 (1)
O(11)	8036 (2)	385 (3)	3570 (2)	41 (1)
B(1)	8574 (3)	722 (5)	2919 (3)	47 (1)
N(1)	8714 (2)	−836 (4)	2541 (2)	51 (1)
C(12)	9213 (4)	−1839 (6)	3151 (4)	82 (2)
C(13)	7816 (4)	−1498 (6)	2190 (3)	72 (2)
C(14)	9260 (4)	−643 (7)	1904 (4)	82 (2)

[a] Equivalent isotropic U defined as one-third of the trace of the orthogonalized U_{ij} tensor.

Table III. Selected Bond Distances and Angles for $[HRu_3(CO)_{10}(\mu\text{-}COBH_2NMe_3)]$ (1)[a]

(a) Bond Distances (Å)			
Ru(1)–Ru(2)	2.823 (1)	H(12)–Ru(1)	1.736 (40)
Ru(1)–Ru(3)	2.832 (1)	H(12)–Ru(2)	1.784 (43)
Ru(2)–Ru(3)	2.835 (1)	C(11)–Ru(1)	1.999 (3)
C(1)–Ru(1)	1.900 (4)	C(11)–Ru(2)	2.010 (3)
C(2)–Ru(1)	1.983 (4)	O(11)–C(11)	1.262 (4)
C(3)–Ru(1)	1.895 (5)	B(1)–O(11)	1.508 (5)
C(4)–Ru(2)	1.898 (5)	H(1)–B(1)	1.096 (46)
C(5)–Ru(2)	1.977 (4)	H(2)–B(1)	1.028 (49)
C(6)–Ru(2)	1.900 (4)	N(1)–B(1)	1.592 (5)
C(7)–Ru(3)	1.913 (4)	C(12)–N(1)	1.475 (7)
C(8)–Ru(3)	1.929 (5)	C(13)–N(1)	1.491 (6)
C(9)–Ru(3)	1.925 (5)	C(14)–N(1)	1.475 (6)
C(10)–Ru(3)	1.947 (4)		
(b) Bond Angles (deg)			
Ru(3)–Ru(1)–Ru(2)	60.2 (1)	C(11)–Ru(1)–Ru(3)	73.9 (1)
C(11)–Ru(1)–Ru(2)	45.4 (1)	Ru(2)–H(12)–Ru(1)	106.6 (22)
C(11)–Ru(1)–C(2)	166.0 (2)	C(11)–Ru(2)–Ru(1)	45.1 (1)
C(11)–Ru(1)–C(3)	93.3 (2)	C(11)–Ru(2)–Ru(3)	73.7 (1)
Ru(3)–Ru(2)–Ru(1)	60.1 (1)	C(11)–Ru(2)–H(12)	78.1 (13)
Ru(2)–Ru(3)–Ru(1)	59.7 (1)	Ru(2)–C(11)–Ru(1)	89.5 (1)
O(11)–C(11)–Ru(1)	132.2 (2)	O(11)–C(11)–Ru(2)	138.1 (3)
B(1)–O(11)–C(11)	125.4 (3)	N(1)–B(1)–H(2)	119.1 (26)
C(12)–N(1)–B(1)	111.4 (4)	H(1)–B(1)–O(11)	99.6 (25)
C(13)–N(1)–B(1)	110.3 (4)	H(2)–B(1)–O(11)	106.0 (26)
H(2)–B(1)–H(1)	113.0 (34)	C(14)–N(1)–B(1)	108.5 (4)
N(1)–B(1)–O(11)	103.7 (3)	N(1)–B(1)–H(1)	112.7 (24)

[a] A labeling scheme is given in Figure 1.

with respect to $\delta = 0$ for Me_4Si and ^{11}B NMR shifts with respect to $\delta = 0$ for $F_3B{\cdot}OEt_2$. All downfield chemical shifts are positive. Infrared spectra were recorded on a Perkin-Elmer FT 1710 spectrophotometer. FAB mass spectra were recorded on a Kratos MS 890 instrument.

All reactions were carried out under argon by using standard Schlenk techniques.[7] Solvents were dried over suitable reagents and freshly distilled under nitrogen before use. The products were separated by centrifugal chromatography with Kieselgel 60-PF$_{254}$ mesh (Merck). $Ru_3(CO)_{12}$ was prepared from $RuCl_3{\cdot}H_2O$ by a literature procedure,[8] and $Ru_3(CO)_{10}(NCMe)_2$ was prepared from $Ru_3(CO)_{12}$ by a published method.[2] The reagents $THF{\cdot}BH_3$ and $Me_3N{\cdot}BH_3$ was used directly as supplied by Aldrich.

Preparation of $[Ru_6(CO)_{17}B][HNMe_3]$ and $HRu_3(CO)_{10}(\mu\text{-}COBH_2NMe_3)$ (1). $Ru_3(CO)_{10}(NCMe)_2$ (ca. 0.13 mmol) was prepared in situ in CH_2Cl_2 (150 mL), from $Ru_3(CO)_{12}$ (0.1 g, 0.16 mmol).[2] $Ru_3(CO)_{11}(NCMe)$ (ca. 0.03 mmol) was also present in solution. The relative amounts of mono- and bis(acetonitrile) derivatives were estimated from solution infrared spectra. To this solution was added $THF{\cdot}BH_3$ (0.5 mmol) at room temperature in the presence of NMe_3 (0.4 mmol). The solution was stirred for 1 h, during which time a color change from yellow to orange occurred, and then evaporated to dryness. The products were separated chromatographically. Eluting with hexane followed by CH_2Cl_2 gave $[HRu_3(CO)_{10}(\mu\text{-}COBH_2NMe_3)]$ as the yellow second fraction (~5% yield); subsequent elution with acetone yielded (~10%) $[Ru_6(CO)_{17}B][HNMe_3]$. $[HRu_3(CO)_{10}(\mu\text{-}COBH_2NMe_3)]$: 250-MHz ^1H NMR ($(CD_3)_2CO$, 298 K) δ 2.56 (s, *Me*), 1.58 (br, B*H*), −14.31 (s, Ru-*H*-Ru); 128-MHz ^{11}B NMR ($(CD_3)_2CO$, 298 K) δ 11.0 (t, J_{BH} = 130 Hz); IR (hexane, cm^{-1}) ν_{BH} 2365 w, 2340 w, ν_{CO} 2096 w, 2055 vs, 2044 s, 2020 vs, 2009 m, 1992 sh; FAB-MS (3-NBA matrix) m/z 686 (P^+). $[Ru_6(CO)_{17}B][HNMe_3]$: 250-MHz ^1H NMR ($(CD_3)_2CO$, 298 K) δ 2.88 (s, *Me*); 128-MHz ^{11}B NMR ($(CD_3)_2CO$, 298 K) δ 202.0 (s, fwhm = 64 Hz, $^{11}B\{^1H\}$ fwhm = 64 Hz); IR ($(CD_3)_2CO$, cm^{-1}) ν_{CO} 2050 w, 2038 w, 2000 m, 1978 sh; FAB-MS (3-NBA matrix) m/z 1096 (P^-).

An alternative route to 1 uses $Me_3N{\cdot}BH_3$ in place of $THF{\cdot}BH_3$ with free amine in solution. Yields of 1 via this route are typically ≤5%.

Crystal Structure Determination. Crystallographic data are collected in Table I. A Stoe-Siemens four-circle diffractometer, using graphite-monochromated Mo Kα radiation (λ = 0.71069 Å), was used for the data collection with a 30-step ω/θ

---

[7] Shriver, D. F.; Drezdon, M. A. *The Manipulation of Air-Sensitive Compounds*, 2nd ed.; Wiley: New York, 1986.

[8] Eady, C. R.; Jackson, P. F.; Johnson, B. F. G.; Lewis, J.; Malatesta, M. C.; MacPartlin, M.; Nelson, W. J. H. *J. Chem. Soc., Dalton Trans.* **1980**, 383.

Scheme I

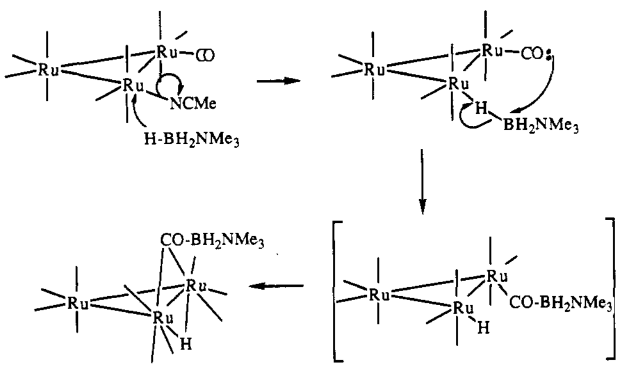

scan mode, with a scan step width of 0.025° and a scan speed varying between 0.5 and 2.0 s per step. The data were corrected for absorption on the basis of 20 ψ-scan reflections (792 data, 10° increments, $8 \leq 2\theta \leq 23°$). The Ru atoms were located by direct methods. All non-hydrogen atoms were refined anisotropically, and all hydrogen atoms (except hydrido and B–H hydrogen atoms) were treated as idealized contributions (d_{C-H} = 1.08 Å). All computations used the SHELX76 program library (G. M. Sheldrick, University of Cambridge, 1976). Table II contains the final atom coordinates, and Table III contains selected bond distances and angles.

MO Calculations. The Fenske–Hall[9] quantum-chemical technique was used to examine the bonding in 1. Atomic coordinates were those determined crystallographically (Table II). Throughout the calculations, the μ-CO bond distance was maintained at 1.26 Å, as observed in 1. This ensured that changes in the bonding within μ-CO as one went from $[HRu_3(CO)_{10}(\mu\text{-}CO)]^-$ to $[HRu_3(CO)_{10}(\mu\text{-}COBH_2NMe_3)]$ were due entirely to the interaction with the borane fragment and were not biased by physically lengthening the C–O bond. For comparative purposes, a calculation was also run on $[HRu_3(CO)_{10}(\mu\text{-}CO)]^-$ with use of the crystallographically determined structure of this anion.[10]

The Fenske–Hall calculations employed single-ζ Slater functions for the 1s and 2s functions of B, C, N, and O. The exponents were obtained by curve-fitting the double-ζ functions of Clementi[11] while maintaining orthogonal functions. The double-ζ functions were used directly for the 2p orbitals. An exponent of 1.16 was used for hydrogen. The Ru functions, chosen for the +1 oxidation state, were augmented by 5s and 5p functions with exponents of 2.20.[12]

Results and Discussion

Synthesis of $[Ru_6(CO)_{17}B][HNMe_3]$ and 1. The reaction of $Ru_3(CO)_{12-x}(NCMe)_x$ (x = 1, 2) with THF·BH_3 in the presence of NMe_3 leads to two boron-containing products. The first product has been characterized spectroscopically and exhibits an extreme downfield ^{11}B NMR chemical shift (δ +202). This, along with the lack of ^{11}B–^1H coupling, implies that the compound contains a metal-encapsulated boron atom, and a formulation of $[Ru_6(CO)_{17}B][HNMe_3]$ is proposed.[13] A related anion, *trans*-$[Fe_4Rh_2(CO)_{16}B]^-$, shows an ^{11}B NMR singal at δ +211,[14] and we have observed that a change from an Fe–B to an Ru–B interaction does not significantly affect the value of the ^{11}B NMR chemical shift.[1,15] The anion $[Ru_6(CO)_{17}B]^-$ is isoelectronic with $Ru_6(CO)_{17}C$ and is expected to have a similar closo structure, viz. an octahedral Ru_6 core with an interstitial main-group atom.[16]

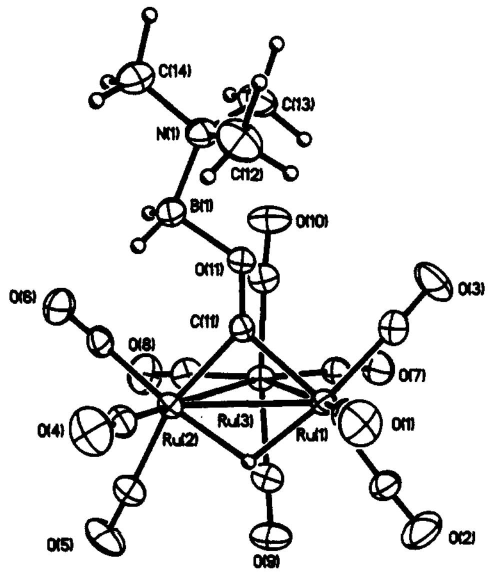

Figure 1. Molecular structure and labeling scheme for 1.

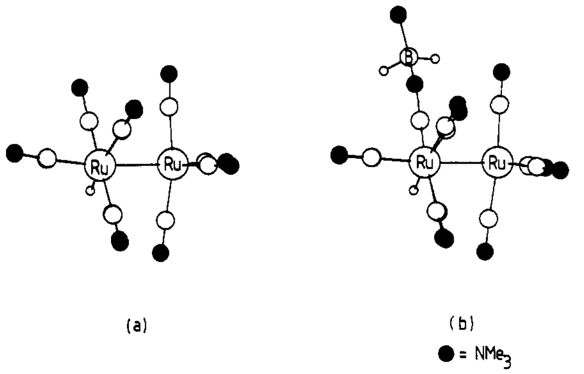

Figure 2. Comparative views of the structures of (a) the $[HRu_3(CO)_{10}(\mu\text{-}CO)]^-$ anion and (b) 1. Each molecule is viewed along the bridged Ru–Ru bond, and the Ru atoms defining this bond are therefore eclipsed. The NMe_3 group in 1 is represented as a single filled circle for clarity.

The second boron-containing product is 1 and may be formulated as L·BH_2(OR) (L = NMe_3; RO = $[HRu_3(CO)_{10}(\mu\text{-}CO)]$). The cluster anion $[HRu_3(CO)_{10}(\mu\text{-}CO)]^-$ functions as a Lewis base toward the boron atom, forming a B–O covalent bond. Thus, 1 is an amine adduct of a substituted borane. During the reaction of $Ru_3(CO)_{12-x}(NCMe)_x$ with L·BH_3 (L = THF, NMe_3), a hydride ligand must be transferred from the original BH_3 fragment to the metal cluster. The mechanism that we envisage (Scheme I) is similar to one suggested by Shore et al. for the generation of $H_3Os_3(CO)_9BCO$ from $H_2Os_3(CO)_{10}$ and diborane in the presence of catalytic amounts of $Me_3N\cdot BH_3$.[17] However, in our case, the reaction sequence terminates with an adduct rather than continues to a cluster product. It seemed to us reasonable that compound 1 might undergo a similar closure to an Ru_3B cluster or might possibly be the precursor to the hexanuclear cluster $[Ru_6(CO)_{17}B]^-$. However, heating 1 in toluene solution for ~5 h produced

---

(9) Hall, M. B.; Fenske, R. F. *Inorg. Chem.* **1972**, *11*, 768.

(10) Johnson, B. F. G.; Lewis, J.; Raithby, P. R.; Süss, G. *J. Chem. Soc., Dalton Trans.* **1979**, 1356.

(11) Clementi, E. *J. Chem. Phys.* **1964**, *40*, 1944.

(12) Richardson, J. W.; Blackman, M. J.; Ranochak, J. F. *J. Chem. Phys.* **1973**, *58*, 3010.

(13) While our paper was in preparation, a report of the crystallographic characterization of $HRu_6(CO)_{17}B$ appeared: Hong, F.-E.; Coffy, T. J.; McCarthy, D. A.; Shore, S. G. *Inorg. Chem.* **1989**, *28*, 3284.

(14) Fehlner, T. P.; Khattar, R.; Puga, J.; Rheingold, A. L. *J. Am. Chem. Soc.* **1989**, *111*, 1877.

(15) Chipperfield, A. K.; Housecroft, C. E.; Rheingold, A. L. *Organometallics*, in press.

(16) Sirugi, A.; Bianchi, M.; Benedetti, E. *J. Chem. Soc. D* **1969**, 596.

(17) Shore, S. G.; Jan, D.-Y.; Hsu, L.-Y.; Hsu, W.-L. *J. Am. Chem. Soc.* **1983**, *105*, 5923.

Table IV. Comparison of the Geometric Parameters for the μ-$COBX_2NR_3$ Unit in 1, $Co_3(CO)_9(\mu_3\text{-}COBH_2NEt_3)$, $Co_3(CO)_9(\mu_3\text{-}COBCl_2NEt_3)$, and $Co_3(CO)_9(\mu_3\text{-}COBBr_2NEt_3)$

	bond param					
compd	*d*(C-O), Å	*d*(O-B), Å	*d*(B-N), Å	∠NBO, deg	∠BOC, deg	ref
1	1.262 (4)	1.508 (5)	1.592 (5)	103.7 (3)	125.4 (3)	*a*
$Co_3(CO)_9(\mu_3\text{-}COBH_2NEt_3)$	1.28 (2)	1.37 (2)	1.66 (2)	105.2 (30)	135.4 (30)	4
$Co_3(CO)_9(\mu_3\text{-}COBCl_2NEt_3)$	1.33	1.42	1.64	105.8	132.4	5[b]
$Co_3(CO)_9(\mu_3\text{-}COBBr_2NEt_3)$	1.31	1.39	1.56	109.7	136.8	6[c]

[a] This work. [b] Average of two crystallographically independent molecules; no esd's given. [c] No esd's given.

Scheme II

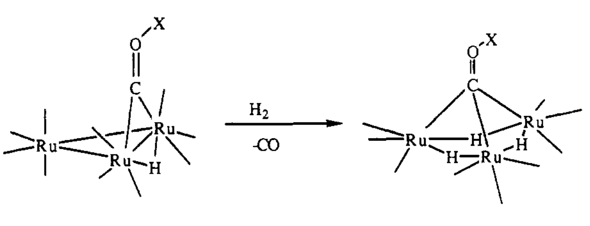

no color change or changes in the solution infrared spectrum.

The reaction scheme outlined in Scheme I assumes that the mono(acetonitrile) cluster $[Ru_3(CO)_{11}(NCMe)]$ is the precursor to the formation of 1 rather than $[Ru_3(CO)_{10}(NCMe)_2]$. Certainly, there is a sufficient quantity of $[Ru_3(CO)_{11}(NCMe)]$ present in the initial solution to account for all the adduct that is formed. On the other hand, displacement of an MeCN ligand by CO may readily occur at any stage during the reaction. We have been unsuccessful in producing $[Ru_3(CO)_{11}(NCMe)]$ in the absence of $[Ru_3(CO)_{10}(NCMe)_2]$. Hence, we are unable to unambiguously assign the precursor to 1.

Molecular Structure of 1. The molecular structure of 1 is shown in Figure 1, and selected bond lengths and angles are listed in Table III. Compound 1 is related to the cluster $[HRu_3(CO)_{10}(\mu\text{-}COMe)]$.[18,19] The three ruthenium atoms in 1 define an equilateral triangle (internal angles 59.7 (1), 60.2 (1), 60.1 (1)°). The spatial distribution of the hydride and carbonyl ligands is almost equivalent to that of the ligands in $[HRu_3(CO)_{10}(\mu\text{-}CO)]^-$[10] and $[HRu_3(CO)_{10}(\mu\text{-}COMe)]$.[18] Figure 2 provides a comparison of the structures of 1 and $[HRu_3(CO)_{10}(\mu\text{-}CO)]^-$. Each is viewed along the bridged Ru-Ru edge (Ru(1)-Ru(2) in Figure 1). The presence of the $[BH_2NMe_3]$ fragment causes a slight distortion to C(6)-O(6); the angle C(11)-Ru(2)-C(6) is 98.0 (2)° as compared to 93.3 (2)° for C(11)-Ru(1)-C(3); corresponding angles in $[HRu_3(CO)_{10}(\mu\text{-}CO)]^-$ are 94.8 (5) and 93.9 (5)°.[10] The μ-C-O bond length is 1 is significantly longer (1.262 (4) Å) than in $[HRu_3(CO)_{10}(\mu\text{-}CO)]^-$ (1.180 (12) Å) but is shorter than in $[HRu_3(CO)_{10}(\mu\text{-}COMe)]$ (1.299 (8) Å). This supports the premise that $[HRu_3(CO)_{10}(\mu\text{-}CO)]^-$ behaves as a Lewis base toward the amine-borane, but the degree of the bond lengthening implies that $[BH_2NMe_3]^+$ is a weaker Lewis acid than $[CH_3]^+$. This is further supported by a decrease in the dihedral angle, α, between the Ru(1)-Ru(2)-C(11) and Ru(1)-Ru(2)-Ru(3) planes along the series $[HRu_3(CO)_{10}(\mu\text{-}CO)]^-$ (α = 102.9°) to 1 (α = 96.7°) to $[HRu_3(CO)_{10}(\mu\text{-}COMe)]$ (α = 94.7°). Keister et al. have illustrated that the rate of conversion from $HRu_3(CO)_{10}(\mu\text{-}COX)$ to $H_3Ru_3(CO)_9(\mu_3\text{-}COX)$ (Scheme II) increases as the Lewis acidity of X increases, i.e. as the π character of the bridging C-O bond is reduced.[19,20]

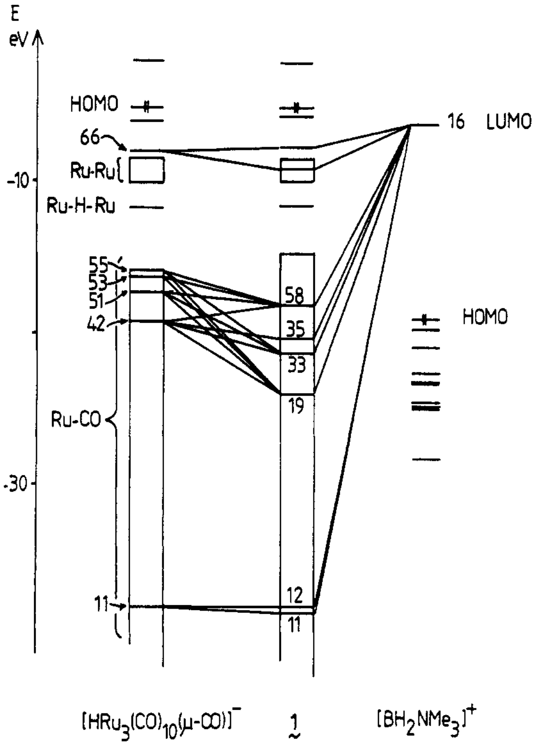

Figure 3. Correlation of the molecular orbitals of the $[HRu_3(CO)_{10}(\mu\text{-}CO)]^-$ and $[BH_2NMe_3]^+$ fragments in 1. Fragment orbital energies are taken from the Fock matrix of complex 1.[21]

Compound 1 is related to $Co_3(CO)_9(\mu_3\text{-}COBH_2NEt_3)$,[4] $Co_3(CO)_9(\mu_3\text{-}COBCl_2NEt_3)$,[5] and $Co_3(CO)_9(\mu_3\text{-}COBBr_2NEt_3)$.[6] Geometrical parameters for the μ-$COBX_2NR_3$ unit in these compounds are listed in Table IV. The bridging C-O bond length in 1 compares favorably with that in $Co_3(CO)_9(\mu_3\text{-}COBH_2NEt_3)$, taking into account the fact that, in the latter cluster, the carbonyl ligand is triply rather than doubly bridging. The further increase in μ-C-O bond length from $Co_3(CO)_9(\mu_3\text{-}COBH_2NEt_3)$ to the halo derivatives is rationalized in terms of the electron-withdrawing effect of the halide substituents relative to the hydrogen atoms. The B-O bond length in 1 of 1.508 (5) Å implies a single bond (sum of the covalent radii 1.51 Å). It is significantly longer than in any of the tricobalt systems, and the B-N bond is correspondingly shorter. The trend is consistent with the differences in carbon-oxygen bond lengths and implied degree of transference of C-O π-electron density. Each of the boron, nitrogen, and carbon atoms of the BH_2NMe_3 unit in 1 is in an approximately tetrahedral environment.

Electronic Structure of 1. The electronic structure of compound 1 has been examined in terms of the inter-

---

(18) Johnson, B. F. G.; Lewis, J.; Orpen, A. G.; Raithby, P. R.; Süss, G. *J. Organomet. Chem.* **1979**, *173*, 187.

(19) Keister, J. B.; Payne, M. W.; Muscatella, M. J. *Organometallics* **1983**, *2*, 219.

(20) Dalton, D. M.; Barnett, D. J.; Duggan, T. P.; Keister, J. B.; Malik, P. T.; Modi, S. P.; Shaffer, M. R.; Smesko, S. A. *Organometallics* **1985**, *4*, 1854.

(21) See for example: Kostic, N. M.; Fenske, R. F. *Inorg. Chem.* **1983**, *22*, 666.

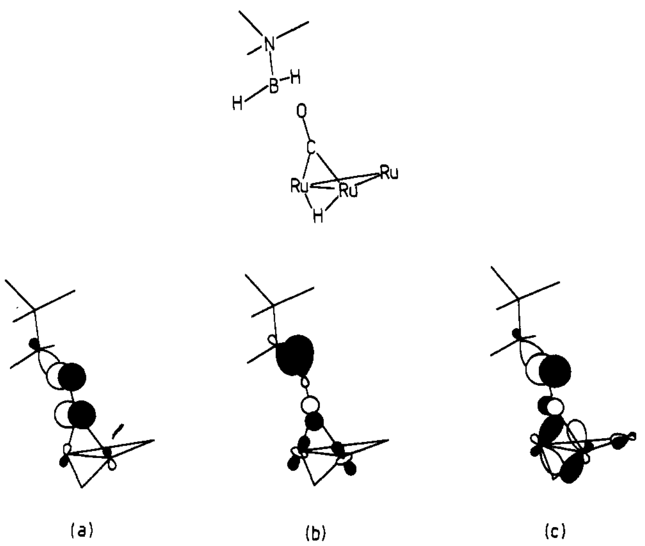

Figure 4. Schematic representations of the principal orbital interactions between the [$HRu_3(CO)_{10}(\mu$-CO)]$^-$ and [BH_2NMe_3]$^+$ fragments on formation of 1: (a) MO 53–MO 16; (b) MO 55–MO 16; (c) MO 66–MO 16.

action of the [$HRu_3(CO)_{10}(\mu$-CO)]$^-$ cluster anion with the [BH_2NMe_3]$^+$ cation. The orbital composition of the [$HRu_3(CO)_{10}(\mu$-CO)]$^-$ fragment is illustrated on the left-hand side of Figure 3. MO's 57–68 possess predominantly metal character, although MO 66 also exhibits 43% bridging carbonyl character.[22] For the [BH_2NMe_3]$^+$ fragment, the only orbital of interest is the LUMO. This is a localized B sp^3 hybrid, which is directed toward the vacant site of the tetrahedral coordination sphere of the boron atom.

Orbital interactions between the [$HRu_3(CO)_{10}(\mu$-CO)]$^-$ and [BH_2NMe_3]$^+$ fragments are shown in Figure 3. The LUMO (MO 16) of the [BH_2NMe_3]$^+$ fragment accepts electron density from MO's 11, 42, 51, 53, 55, and 66 of the triruthenium anion. The latter comprise six of the seven[23] occupied MO's in [$HRu_3(CO)_{10}(\mu$-CO)]$^-$ that exhibit μ-CO character. The seventh is MO 54. The low-lying MO 11 is σ_{CO} bonding and possesses 68% oxygen atom 2s character. MO's 42 and 51/55 are σ^*_{CO} and σ_{CO} orbitals, respectively, but more importantly, each exhibits oxygen atom lone-pair character. In each case, the orientation of the lone pair is approximately collinear with the O–C vector, implying that the oxygen atom is essentially sp hybridized. Fragment MO's 53 and 54 correspond to the set of π_{CO} bonding orbitals, while MO 66 is the antibonding analogue of MO 53. (MO 66 is stabilized by virtue of Ru–μ-CO bonding character. The remaining π^*_{CO} orbital is identified as the unoccupied MO 73.)

Of the total Mulliken overlap between MO's 11, 42, 51, 53, 55, and 66 with the MO 16 of the amine–borane, 87% is attributable to the three interactions depicted in Figure 4. The π_{CO} orbital, MO 53, lies parallel to the Ru(1)–Ru(2) bond and is beautifully set up to interact with the LUMO of the [BH_2NMe_3]$^+$ fragment to generate a B–O σ-bond. Note, however, that a similar interaction involving the second π_{CO} orbital, MO 54, is disallowed by symmetry. There is a net transfer of 0.63 electron from [$HRu_3(CO)_{10}(\mu$-CO)]$^-$ to [BH_2NMe_3]$^+$ on forming 1, and consequential μ-CO bond weakening occurs as electrons are removed from the σ_{CO} and π_{CO} MO's. This is offset to a small extent by the loss of electrons from MO 66 (π^*_{CO}). Hence, even under the constraint of a fixed μ-C–O bond length, the electronic factors that lead to a lowering of the C–O bond order are evident.

To what extent, if any, is the bonding within the triruthenium carbonyl cluster framework perturbed by interaction with the borane? Of the [$HRu_3(CO)_{10}(\mu$-CO)]$^-$ fragment orbitals that interact with the amine–borane, MO 66 is the only one that exhibits significant metal character; MO's 53 and 55 exhibit <6% per Ru atom (Figure 4). We have previously illustrated that the primary interaction between a trimetal framework and a μ_2-bridging ligand involves the tangential π-orbital on the bridgehead atom;[24] i.e. in this case, MO 66 is the relevant orbital. In going from the [$HRu_3(CO)_{10}(\mu$-CO)]$^-$ fragment to 1, the occupancy of MO 66 is reduced from 2.00 to 1.88 electrons, and a net 21% decrease in the Mulliken overlap population between atoms Ru(1), or Ru(2), and C(11) is observed. Significantly, if we compare the experimental structures of the [$HRu_3(CO)_{10}(\mu$-CO)]$^-$ anion[10] and 1, *no* corresponding increase in bond lengths is observed. In our fragment analysis, the dihedral angle between the Ru(1)–Ru(2)–C(11) and Ru(1)–Ru(2)–Ru(3) planes remains constant. However, in practice, this angle decreases in going from [$HRu_3(CO)_{10}(\mu$-CO)]$^-$ to 1. The analysis of the electronic structure of 1 in relation to that of the free [$HRu_3(CO)_{10}(\mu$-CO)]$^-$ anion suggests that the shift in the position of the bridging carbonyl group occurs in order to restore the metal–bridgehead bonding. The metal–bridgehead π-interaction will eventually evolve into one of the M_3C π-bonding interactions which are primary bonding MO's between a trimetal framework and a μ_3-bridging ligand.[25-28]

In conclusion, the molecular orbital calculations support the experimental observation that the [$HRu_3(CO)_{10}(\mu$-CO)]$^-$ anion acts as a Lewis base toward the amine–borane and also indicate why subtle structural changes occur to the trimetal cluster framework.

Acknowledgment is made to the donors of the Petroleum Research Fund, administered by the American Chemical Society, for support of this research, to the Royal Society for a 1983 University Research Fellowship (to C.E.H.), and to Johnson-Matthey for generous loans of $RuCl_3$. We also wish to thank Professor Jerry Keister for useful discussions.

Supplementary Material Available: Tables of atomic coordinates, bond distances, bond angles, thermal parameters, and H atom coordinates (5 pages); a listing of structure factors (21 pages). Ordering information is given on any current masthead page.

---

(22) The MO's of [$HRu_3(CO)_{10}(\mu$-CO)]$^-$ are only marginally perturbed as the structure is changed from the true experimental geometry to that observed for this fragment in 1; MO 66 (π^*_{CO}) is stabilized, and each of the C–O bonding MO's is destabilized, consistent with the elongation of the μ-C–O bond.

(23) Minor μ-CO contributions are found in several additional occupied MO's of the [$HRu_3(CO)_{10}(\mu$-CO)]$^-$ fragment. The seven MO's considered each contain ≥43% CO character.

(24) Housecroft, C. E.; Owen, S. M. *Organometallics* **1988**, *7*, 1387.

(25) Schilling, B. E. R.; Hoffmann, R. *J. Am. Chem. Soc.* **1979**, *101*, 3456.

(26) Sherwood, D. E.; Hall, M. B. *Organometallics* **1982**, *1*, 1519.

(27) Barreto, R. D.; Fehlner, T. P.; Hsu, L.-Y.; Jan, D.-Y.; Shore, S. G. *Inorg. Chem.* **1986**, *25*, 3572.

(28) Lynam, M. M.; Chipman, D. M.; Barreto, R. D.; Fehlner, T. P. *Organometallics* **1987**, *6*, 2405.